Excluded-Volume Effects on the Hydrodynamic Radius of Oligo- and Polyisobutylenes in Dilute Solution

Masashi Osa, Fumiaki Abe, Takenao Yoshizaki, Yoshiyuki Einaga, and Hiromi Yamakawa*

Department of Polymer Chemistry, Kyoto University, Kyoto 606-01, Japan

Received August 29, 1995; Revised Manuscript Received November 20, 1995[⊗]

ABSTRACT: The translational diffusion coefficient D was determined from dynamic light scattering measurements for oligo- and polyisobutylenes in isoamyl isovalerate (IAIV) at 25.0 °C (Θ) and in *n*-heptane at 25.0 °C in the range of weight-average molecular weight M_w from 1.01×10^3 to 1.76×10^6. The values of the unperturbed and perturbed hydrodynamic radii $R_{H,\Theta}$ and R_H defined from D in IAIV and in *n*-heptane, respectively, were found to agree with each other in the oligomer region, indicating that the values of $R_{H,\Theta}$ may be adopted as those of the unperturbed hydrodynamic radius $R_{H,0}$ in *n*-heptane at 25.0 °C. The values of the hydrodynamic-radius expansion factor α_H in *n*-heptane at 25.0 °C are then obtained as the ratio $R_H/R_{H,\Theta}$ from those values thus determined. The data for $R_{H,\Theta}$ are analyzed as usual by the use of the corresponding (unperturbed) helical wormlike (HW) chain theory. The results for α_H as a function of the scaled excluded-volume parameter $\tilde{z}$ defined in the Yamakawa−Stockmayer−Shimada theory for the HW chain with excluded volume are consistent with the previous results for atactic polystyrene and poly(dimethylsiloxane). The implication is that the quasi-two-parameter scheme may be valid for α_H as well as for the gyration-radius and viscosity-radius expansion factors α_S and α_η irrespective of the differences in chain stiffness, local conformation, and solvent condition. It is again found that the Barrett equation overestimates α_H. This disagreement between theory and experiment may be qualitatively explained by the Yamakawa−Yoshizaki theory, which takes account of the possible effect of fluctuating hydrodynamic interaction on α_H. It is also again found that α_H coincides with α_η within experimental error over the whole range of M_w studied.

Introduction

In recent experimental papers of this series on the excluded-volume effects in dilute solutions of oligomers and polymers,[1] we have reported some results for the hydrodynamic-radius expansion factor α_H for the hydrodynamic radius R_H defined from the translational diffusion coefficient D for atactic polystyrene (a-PS)[2,3] and poly(dimethylsiloxane) (PDMS).[4] It has then been shown that the quasi-two-parameter (QTP) scheme is valid for α_H as well as for the gyration-radius[1,5,6] and viscosity-radius[4−8] expansion factors α_S and α_η; these expansion factors may be expressed as functions only of the scaled excluded-volume parameter $\tilde{z}$ defined in the Yamakawa−Stockmayer−Shimada (YSS) theory[9−11] that takes account of the effects of excluded volume and chain stiffness on the basis of the helical wormlike (HW) chain model,[12,13] irrespective of the differences in chain stiffness, local conformation, and solvent condition. In the present paper, we proceed to make a study of α_H for polyisobutylene (PIB) along the same line as in the previous papers[2−4] in order to examine the validity of the above QTP scheme for PIB.

For this polymer, we have already investigated the intrinsic viscosities $[\eta]_\Theta$ in the unperturbed (Θ) state, i.e., in isoamyl isovalerate (IAIV) at 25.0 °C and in benzene at 25.0 °C,[14] and also $[\eta]$ in the good solvent *n*-heptane at 25.0 °C,[7] and found that $[\eta]_\Theta$ becomes negative[14] for the oligomers with very small molecular weight M as in the case of PDMS.[15] Although the negative $[\eta]$ may be regarded as arising from specific interactions between solute and solvent molecules, there is a difference in the situation between the two polymers. In the case of PDMS, the so-called draining effect exists besides the negative $[\eta]$, and then the hydrodynamic chain thickness determined from $[\eta]_\Theta$ and D_Θ by the use of the corresponding HW theories becomes very small, and moreover, it depends appreciably on solvent.[15] This dependence as well as the negative $[\eta]$ had therefore to be taken into account in order to determine α_H and α_η correctly.[4] On the other hand, there is no evidence of the draining effect for PIB, and the value of its chain thickness determined after the removal of the effect of the specific interactions on $[\eta]_\Theta$ seems reasonable compared to the one estimated from its chemical structure. Further, for PIB oligomer samples in the range of M from 6.41×10^2 to 1.81×10^3, where the latter effect in IAIV may be regarded as negligibly small if any,[14] the values of $[\eta]$ in *n*-heptane have been found to agree well with those in IAIV at Θ,[7] so that α_η in the good solvent *n*-heptane has been able to be calculated by adopting $[\eta]_\Theta$ in IAIV as the unperturbed value $[\eta]_0$ in *n*-heptane. Thus, in the present study, we also use *n*-heptane and IAIV as good and Θ solvents, respectively, to determine α_H.

We have already carried out dynamic light scattering (DLS) measurements for PIB in the range of large M ($\gtrsim 4 \times 10^5$) in IAIV at Θ in order to determine D_Θ (and the transport factor ρ).[16] Thus we first determine its values in IAIV at Θ over a wider range of M, including the oligomers, and analyze these present and previous data together by the use of the HW theory of D_Θ.

Experimental Section

Materials. Most of the PIB samples used in this work are the same as those used in the previous studies of $[\eta]_\Theta$,[14] $[\eta]$,[7] and the transport factors ρ and Φ.[16] The samples with the weight-average molecular weight $M_w > 5 \times 10^3$ are the fractions separated by fractional precipitation from the commercial samples of Enjay Chemical Co., named Vistanex LM-MS, L-80, and L-200. The oligomer samples with $M_w < 5 \times 10^3$ are the fractions separated by preparative gel permeation chromatography (GPC) from the original samples prepared by living cationic polymerization and then subjected to dehydrochlorination to remove the terminal chlorine atom. The three

[⊗] Abstract published in *Advance ACS Abstracts,* February 15, 1996.

0024-9297/96/2229-2302$12.00/0

Table 1. Values of M_w, x_w, and M_w/M_n for Oligo- and Polyisobutylenes

sample	M_w	x_w	M_w/M_n
OIB18[a]	1.01×10^3	18.0	1.02
OIB26a	1.56×10^3	27.9	1.01
PIB2a	1.81×10^4	323	1.08
PIB5	4.85×10^4	866	1.06
PIB13a	1.39×10^5	2480	1.07
PIB40[b]	4.22×10^5	7540	1.09
PIB60	6.34×10^5	11300	1.06
PIB80	8.19×10^5	14600	1.09
PIB180	1.76×10^6	31400	1.09

[a] M_ws of OIB18 and PIB5 had been determined from SLS in *n*-heptane at 25.0 °C.[14] [b] M_ws of PIB40 through PIB180 had been determined from SLS in IAIV at 25.0 °C.[7,16]

samples OIB26, PIB2, and PIB13 previously[7,14] used had been contaminated somewhat in the course of measurements carried out repeatedly in the previous studies, so that we refractionated OIB26 by preparative GPC, and PIB2 and PIB13 by fractional precipitation. As a result, the values of M_w for these reprepared samples, which we designate as OIB26a, PIB2a, and PIB13a, corresponding to OIB26, PIB2, and PIB13, respectively, became somewhat different from those for the latter, so that we redetermined the former M_w from static light scattering (SLS) measurements as described in a later subsection.

The values of M_w, the weight-average degree of polymerization x_w calculated from M_w, and the ratio of M_w to the number-average molecular weight M_n determined by analytical GPC are listed in Table 1. As seen from the values of M_w/M_n, all the samples are sufficiently narrow in molecular weight distribution. Note that all the samples used in this work have the fixed chemical structures at their chain ends independent of M_w, and there is no disorder in their main chain sequences such as branching and dislocation of the methyl side groups, as previously[14] mentioned.

The solvent IAIV (Tokyo Kasei Kogyo Co.) was purified by distillation under reduced pressure after dehydration with potassium carbonate. The other solvent *n*-heptane was purified according to a standard procedure.

Dynamic Light Scattering. DLS measurements were carried out to determine D_Θ for six samples in IAIV at 25.0 °C (Θ) and D for all the samples in *n*-heptane at 25.0 °C by the use of a Brookhaven Instruments Model BI-200SM light scattering goniometer with vertically polarized incident light of 488 nm wavelength from a Spectra-Physics Model 2020 argon ion laser equipped with a Model 583 temperature-stabilized etalon for single-frequency-mode operation. The photomultiplier tube used was EMI 9863B/350, the output from which was processed by a Brookhaven Instruments Model BI2030AT autocorrelator with 264 channels. (An electric shutter was attached to the original detector alignment in order to monitor the dark count automatically). The normalized autocorrelation function $g^{(2)}(t)$ of the scattered light intensity $I(t)$ at time t was measured at four or five concentrations and at scattering angles θ ranging from 16 to 50°.

From the data for $g^{(2)}(t)$ thus determined at finite mass concentrations c, we determine D at an infinitely long time[15] at infinite dilution in the same manner as that used in the previous studies.[2−4,15−18] At small c, the plot of $(1/2)\ln[g^{(2)}(t) - 1]$ against t in general follows a straight line represented by

$$(1/2)\ln[g^{(2)}(t) - 1] = \text{const} - At \tag{1}$$

with A the slope for such large t that all the internal motions of solute polymer chains have relaxed away.[15] With the slope A evaluated from the plot, we may determine the apparent diffusion coefficient $D^{(LS)}(c)$ at finite c from

$$D^{(LS)}(c) = \lim_{k\to 0} A/k^2 \tag{2}$$

where k is the magnitude of the scattering vector and is given by

$$k = (4\pi/\tilde{\lambda})\sin(\theta/2) \tag{3}$$

with $\tilde{\lambda}$ the wavelength of the incident light in the solvent. At sufficiently small c, $D^{(LS)}(c)$ may be expanded as

$$D^{(LS)}(c) = D^{(LS)}(0)(1 + k_D^{(LS)}c + ...) \tag{4}$$

so that the desired $D = D(\infty)$ (at an infinitely long time) may be determined from extrapolation of $D^{(LS)}(c)$ to $c = 0$ as

$$D = D^{(LS)}(0) \tag{5}$$

The most concentrated solution of each sample in IAIV was prepared gravimetrically and made homogeneous by continuous stirring at ca. 50 °C for 3−4 days, and the one in *n*-heptane was similarly prepared and was stirred at room temperature for 1 day. They were optically purified by filtration through a Teflon membrane of pore size 0.10−0.45 μm. The solutions of lower concentrations were obtained by successive dilution. The polymer mass concentrations c of the test solutions were calculated from the weight fractions with the densities of the solutions.

The values of the refractive index at 488 nm and the viscosity coefficient η_0 used are 1.415 and 1.33 cP, respectively, for pure IAIV at 25.0 °C and 1.390 and 0.392 cP, respectively, for pure *n*-heptane at 25.0 °C.

Static Light Scattering. SLS measurements were carried out in *n*-heptane at 25.0 °C to determine M_w for the samples OIB26a, PIB2a, and PIB13a. The apparatus system, experimental procedure, and method of data analysis are the same as those described in the previous paper.[14]

The value of the refractive index increment $\partial n/\partial c$ measured with a Shimadzu differential refractometer at 436 nm is 0.1403 for OIB26a in *n*-heptane at 25.0 °C. The values of $\partial n/\partial c$ used for the other samples in *n*-heptane at 25.0 °C are 0.1435 (independent of M_w).

Viscosity. Viscosity measurements were also carried out for the samples OIB26a, PIB2a, and PIB13a in IAIV at Θ and in *n*-heptane at 25.0 °C in order to evaluate α_η for them in *n*-heptane. Note that the values of α_η for the other samples in *n*-heptane at 25.0 °C had already been determined.[7] We used conventional capillary and four-bulb spiral capillary viscometers of the Ubbelohde type. In all the measurements, the flow time was measured to a precision of 0.1 s, keeping the difference between those of the solvent and solution larger than ca. 20 s. In the measurements for the IAIV solutions, the surface of the water in a thermostat was covered with liquid paraffin as before[14] to remove the possible effects of moisture. The test solutions were maintained at constant temperature within ±0.005 °C during the measurements. The data obtained were treated as usual by the Huggins and Fuoss−Mead plots to determine $[\eta]$ and the Huggins coefficient k'.

The test solutions were prepared in the same manner as in the case of DLS measurements. Density corrections were made in the calculations of c and also of the relative viscosity from the flow times of the solution and solvent.

Results

Translational Diffusion Coefficient. Although the results are not explicitly shown here, the data points for $(1/2)\ln[g^{(2)}(t) - 1]$ plotted against t at any k examined were found to follow a straight line over the whole range of t studied, exhibiting no curvature due to the internal motions of the chain, and the ratio A/k^2 determined from its slope was found to be independent of k within experimental error in the range of k studied, for all molecular weights, solvents, and concentrations. Thus the value of $D^{(LS)}(c)$ $[=(A/k^2)_{k=0}]$ at a given finite c was determined as the mean of the observed values of A/k^2 for each sample in each solvent.

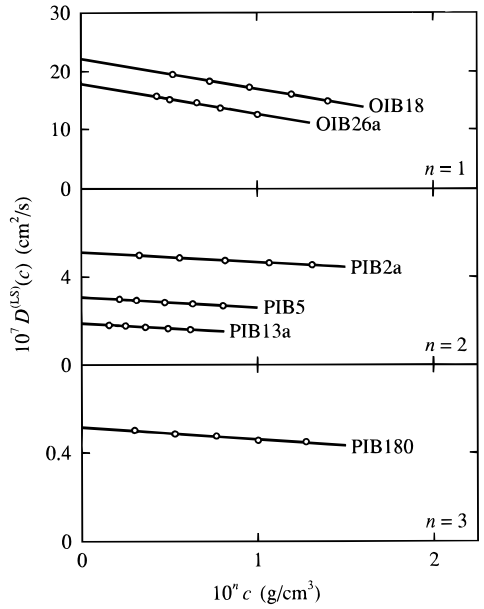

Figure 1. Plots of $D^{(LS)}(c)$ against c for the PIB samples indicated in IAIV at 25.0 °C.

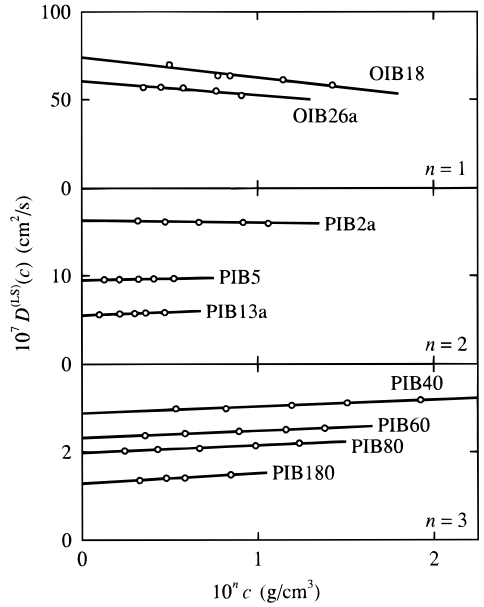

Figure 2. Plots of $D^{(LS)}(c)$ against c for the PIB samples indicated in *n*-heptane at 25.0 °C.

Figures 1 and 2 show plots of $D^{(LS)}(c)$ against c for all the samples in IAIV at Θ and in *n*-heptane at 25.0 °C, respectively. The data points for each sample are seen to follow a straight line, and thus $D^{(LS)}(0)$ (=D) and $k_D^{(LS)}$ may be accurately determined from its ordinate intercept and slope, respectively. It is also seen that the values of $k_D^{(LS)}$ for all the samples in IAIV at Θ are negative, while those in *n*-heptane are positive except for the three samples with the lowest M_w.

The values of D_Θ and $k_D^{(LS)}$ thus obtained for all the PIB samples in IAIV at Θ are given in Table 2 along with the unperturbed values $R_{H,\Theta}$ of R_H calculated from the defining equation,

$$R_H = k_B T/6\pi\eta_0 D \qquad (6)$$

where k_B is the Boltzmann constant, T is the absolute temperature, and η_0 is the viscosity coefficient of the solvent. The values of D_Θ for the samples PIB40, PIB60, and PIB80 have been reproduced from ref 16, and those of $k_D^{(LS)}$ for these samples are the ones determined therein (although not reported). The values of D, $k_D^{(LS)}$, and R_H similarly obtained for all the PIB samples in *n*-heptane at 25.0 °C are given in Table 3.

Table 2. Results of DLS Measurements for Oligo- and Polyisobutylenes in IAIV at 25.0 °C (Θ)

sample	$10^8 D_\Theta$, cm²/s	$k_D^{(LS)}$, cm³/g	$R_{H,\Theta}$, Å
OIB18	222	$-2._3$	7.42
OIB26a	178	$-2._9$	9.21
PIB2a	51.1	$-8._7$	32.1
PIB5	30.8	−16	53.3
PIB13a	18.9	−24	86.7
PIB40[a]	10.6	−47	155
PIB60	8.55	−64	192
PIB80	7.52	−80	218
PIB180	5.16	−110	318

[a] The values of D_Θ of PIB40 through PIB80 have been reproduced from ref 16.

Table 3. Results of DLS Measurements for Oligo- and Polyisobutylenes in *n*-Heptane at 25.0 °C

sample	$10^8 D$, cm²/s	$k_D^{(LS)}$, cm³/g	R_H, Å
OIB18	741	$-1._6$	7.52
OIB26a	604	$-1._3$	9.23
PIB2a	163	$-1._5$	34.2
PIB5	95.0	$3._5$	58.6
PIB13a	55.0	13	101
PIB40	28.8	56	194
PIB60	23.3	68	240
PIB80	19.9	88	281
PIB180	12.9	180	432

Figure 3 shows double-logarithmic plots of $R_H/M_w^{1/2}$ (in Å) against M_w for PIB in *n*-heptane at 25.0 °C (unfilled circles) and in IAIV at Θ (filled circles). It is seen that the ratio $R_{H,\Theta}/M_w^{1/2}$ in IAIV is almost independent of M_w over the whole range of M_w studied, while $R_H/M_w^{1/2}$ in *n*-heptane increases monotonically with increasing M_w except in the oligomer region, and that the difference between their values, i.e., the excluded-volume effect on R_H in *n*-heptane at 25.0 °C becomes appreciable for $M_w \gtrsim 10^4$. The values of R_H for the two oligomer samples with the lowest M_w in *n*-heptane at 25.0 °C agree with the corresponding values in IAIV at Θ as in the case of $[\eta]$ previously[7] studied. This agreement implies that the unperturbed value $R_{H,0}$ for the PIB chain in *n*-heptane at 25.0 °C may be considered to be identical with the value of $R_{H,\Theta}$ in IAIV at Θ. We may then evaluate α_H correctly for PIB in *n*-heptane by the use of the values of $R_{H,\Theta}$ in IAIV as the reference standards.

For comparison, the literature data due to Fetters et al.[19] for PIB in the same solvents, i.e., in *n*-heptane at 25.0 °C (unfilled triangles) and in IAIV at 22.1 °C (filled triangles), are also plotted in Figure 3. It is seen that their results and ours in *n*-heptane agree with each other within experimental error, while their values in IAIV are somewhat larger than ours. Note that the Θ temperature 22.1 °C adopted by them is somewhat lower than our value 25.0 °C.

Intrinsic Viscosity. The results for $[\eta]$ (and $[\eta]_\Theta$) and k' for the three reprepared PIB samples in *n*-heptane at 25.0 °C and in IAIV at Θ are summarized in Table 4. These values of $[\eta]$ and $[\eta]_\Theta$ are used for the calculation of α_η in the next section.

Discussion

Analysis of $R_{H,\Theta}$ on the Basis of the HW Model. We first analyze the data for $R_{H,\Theta}$ (or D_Θ) as usual on

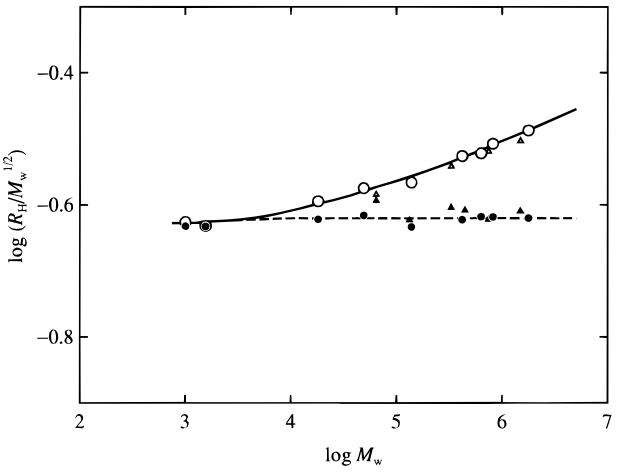

Figure 3. Double-logarithmic plots of $R_H/M_w^{1/2}$ (in Å) against M_w for PIB: (○) in *n*-heptane at 25.0 °C (present data); (●) in IAIV at 25.0 °C (Θ) (present data); (△) in *n*-heptane at 25.0 °C (Fetters et al.);[19] (▲) in IAIV at 22.1 °C (Fetters et al.).[19] The solid and dashed curves connect smoothly the present data points in *n*-heptane and IAIV, respectively.

Table 4. Results of Viscometry for Oligo- and Polyisobutylenes in *n*-Heptane at 25.0 °C and IAIV at 25.0 °C (Θ)

	n-heptane, 25.0 °C		IAIV, 25.0 °C (Θ)	
sample	$[\eta]$, dL/g	k'	$[\eta]_\Theta$, dL/g	k'
OIB26a	0.0456	0.74	0.0443	0.60
PIB2a	0.172	0.43	0.141	0.55
PIB13a	0.620	0.37	0.394	0.52

the basis of the HW touched-bead model.[17] The HW chain itself may be described in terms of the four basic model parameters: the differential-geometrical curvature κ_0 and torsion τ_0 of its characteristic helix taken at the minimum zero of its elastic energy, the static stiffness parameter λ^{-1}, and the shift factor M_L as defined as the molecular weight per unit contour length. For the touched-bead model chain of total contour length $L = Nd_b$, with N the number of beads in the chain and d_b the diameter of the bead, the quantity $M_w/6\pi R_{H,\Theta}$ ($=\eta_0 D_\Theta M_w/k_B T$), which is proportional to the sedimentation coefficient, may be written in the form

$$M_w/6\pi R_{H,\Theta} = (M_L/3\pi) f_D(\lambda L;\lambda^{-1}\kappa_0,\lambda^{-1}\tau_0,\lambda d_b) \quad (7)$$

where the function f_D is given by eq 6 of ref 17 and may be evaluated numerically by the use of the interpolation formula for the mean reciprocal of the end-to-end distance of the chain as given in the Appendix of ref 20. The function f_D satisfies the following asymptotic relation,

$$\lim_{\lambda L\to\infty} f_D(\lambda L)/(\lambda L)^{1/2} = (\sqrt{6}/2) c_\infty^{-1/2} \rho_\infty \quad (8)$$

where

$$c_\infty = \lim_{\lambda L\to\infty} (6\lambda\langle S^2\rangle_0/L) = \frac{4 + (\lambda^{-1}\tau_0)^2}{4 + (\lambda^{-1}\kappa_0)^2 + (\lambda^{-1}\tau_0)^2} \quad (9)$$

with $\langle S^2\rangle_0$ the unperturbed mean-square radius of gyration, and ρ_∞ denotes the (theoretical) coil-limiting value of the ratio ρ of $\langle S^2\rangle_0^{1/2}$ to $R_{H,\Theta}$ and is equal to the Kirkwood value 1.505 (for the unperturbed chain).

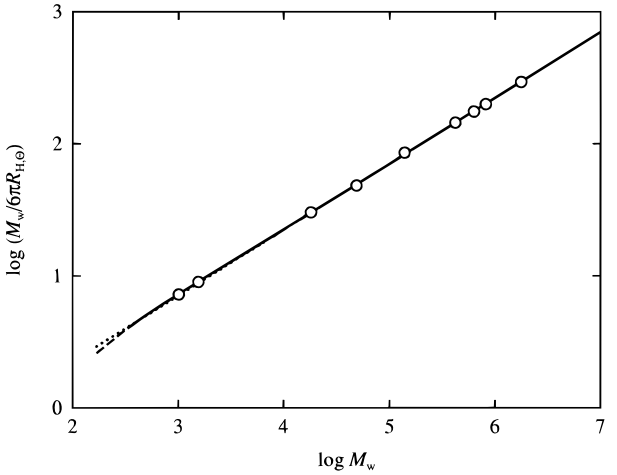

Figure 4. Double-logarithmic plots of $M_w/6\pi R_{H,\Theta}$ (in Å^{-1}) against M_w for PIB in IAIV at 25.0 °C (Θ). The solid curve represents the best-fit HW theoretical values for $N \geq 2$, the dashed line segment connecting the values for $N = 1$ and 2. The dotted straight line has a slope of 0.5.

Table 5. Values of the HW Model Parameters for Polyisobutylene in IAIV at 25.0 °C (Θ)

$\lambda^{-1}\kappa_0$	λ^{-1}, Å	M_L, Å^{-1}	d_b, Å	obsd quantity
0	18.7	24.1	6.9	D_Θ
0	12.7	24.1	6.4	$[\eta]_\Theta$[a]

[a] Reproduced from ref 14.

The basic equations required for the analysis of the data may then be written as

$$\log(M_w/6\pi R_{H,\Theta}) = \log f_D(\lambda L) + \log M_L - 0.975 \quad (10)$$

$$\log M_w = \log(\lambda L) + \log(\lambda^{-1} M_L) \quad (11)$$

Thus the quantities M_L and $\lambda^{-1}M_L$ may be estimated from a best fit of double-logarithmic plots of the theoretical f_D against λL for properly chosen values of $\lambda^{-1}\kappa_0$, $\lambda^{-1}\tau_0$, and λd_b to that of the observed $M_w/6\pi R_{H,\Theta}$ against M_w, so that we may in principle determine $\lambda^{-1}\kappa_0$, $\lambda^{-1}\tau_0$, λ^{-1}, M_L, and d_b. However, it is impossible to determine unambiguously all five of these parameters by the above curve fitting, since the experimental double-logarithmic plot of $M_w/6\pi R_{H,\Theta}$ against M_w follows its asymptotic straight line of slope $^1/_2$ almost over the whole range of M_w studied as in the corresponding plot of $[\eta]_\Theta$ against M_w for PIB in IAIV (and also in benzene) at Θ.[14] Therefore, considering as before[14] that the PIB chain may be represented by the Kratky−Porod (KP) wormlike chain,[21] i.e., the HW chain with $\kappa_0 = 0$ (so that τ_0 is undetermined), and has the same value of M_L as that for the 8_3 helix in the crystalline state,[22] i.e., $M_L = 24.1$ Å^{-1}, we determine the remaining two parameters λ^{-1} and d_b.

In Figure 4, the present data for $M_w/6\pi R_{H,\Theta}$ (in Å^{-1}) for PIB in IAIV at 25.0 °C (Θ) are double-logarithmically plotted against M_w. The solid curve represents the best-fit theoretical values calculated for $N \geq 2$ from eq 7 with $\lambda d_b = 0.37$ and $\log(\lambda^{-1}M_L) = 2.653$, the dashed line segment connecting those values for $N = 1$ and 2. It is seen that the theory may reproduce well the experimental results. The values of the HW model parameters thus determined are listed in the first row of Table 5. In the second row there are also given the values previously determined from $[\eta]_\Theta$.[14] The value 18.7 Å of λ^{-1} determined from D_Θ is larger than that from $[\eta]_\Theta$.

Table 6. Values of α_H, α_S, and α_η for Oligo- and Polyisobutylenes in *n*-Heptane at 25.0 °C

sample	α_H	α_S[a]	α_η[b]
OIB18	1.01		1.01
OIB26a	1.00		1.01
PIB2a	1.07		1.07
PIB5	1.10		1.11
PIB13a	1.17		1.16
PIB40	1.25	1.27	1.24
PIB60	1.25	1.31	1.27
PIB80	1.29	1.37	1.30
PIB180	1.36	1.46	1.37

[a] The values of α_S have been reproduced from ref 7. [b] The values of α_η have been reproduced from ref 7 except for OIB26a, PIB2a, and PIB13a (present data).

We note that this is the case with the other polymers previously[15,17,18,23] studied. As mentioned in the previous papers,[17,18] it may be regarded as arising from the disagreement between the theoretical and experimental values of ρ_∞ and the Flory−Fox factor Φ_∞ (in the coil limit). However, the difference between the two values of λ^{-1} (from D_Θ and $[\eta]_\Theta$) for PIB is somewhat larger than those for the other polymers.[15,17,18,23]

Relations of α_H to α_S and α_η. In table 6 are summarized the values of α_H calculated for the PIB samples in *n*-heptane at 25.0 °C from the equation

$$R_H = R_{H,\Theta}\alpha_H \tag{12}$$

with the values of R_H and $R_{H,\Theta}$ given in Tables 3 and 2, respectively. As mentioned in the Results section, it has been confirmed that the relation $R_{H,0} = R_{H,\Theta}$ holds for the present polymer−solvent system. In the table the values of α_S and α_η in *n*-heptane have also been reproduced from ref 7 except for those of α_η for the three samples OIB26a, PIB2a, and PIB13a, which have been calculated from the equation

$$[\eta] = [\eta]_\Theta \alpha_\eta^{\ 3} \tag{13}$$

with the values of $[\eta]$ and $[\eta]_\Theta$ given in Table 4. As mentioned in the Introduction, it had already been confirmed that the relation $[\eta]_0 = [\eta]_\Theta$ also holds for this polymer−solvent system.[7] Recall that small-angle X-ray scattering measurements are not feasible to determine $\langle S^2\rangle_\Theta$ for PIB in IAIV because of the extremely low excess electron density,[14] so that the values of α_S for the samples with $M_w < 2 \times 10^5$ are not available.

Figure 5 shows double-logarithmic plots of α_H against α_S for PIB in *n*-heptane at 25.0 °C (unfilled circles). For comparison, it also includes the previous results for a-PS in toluene at 15.0 °C (bottom-half-filled circles),[2] in 4-*tert*-butyltoluene at 50.0 °C (top-half-filled circles),[2] and in cyclohexane at 36.0−45.0 °C (squares).[3] (Fetters et al.[19] have not obtained data for α_S corresponding to those for $R_{H,\Theta}$ and R_H plotted in Figure 3.) The dotted curve represents the values calculated from the Barrett equation[24] for α_H,

$$\alpha_H = (1 + 6.09z + 3.59z^2)^{0.1} \tag{14}$$

and the Domb−Barrett equation[25] for α_S,

$$\alpha_S^{\ 2} = [1 + 10z + (70\pi/9 + 10/3)z^2 + 8\pi^{3/2}z^3]^{2/15} \times [0.933 + 0.067\exp(-0.85z - 1.39z^2)] \tag{15}$$

with z the conventional excluded-volume parameter. The solid curve represents the values calculated from

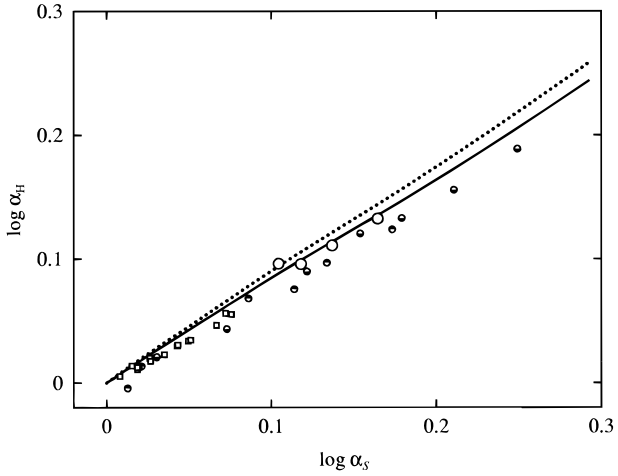

Figure 5. Double-logarithmic plots of α_H against α_S: (○) for PIB in *n*-heptane at 25.0 °C (present data); (◒) for a-PS in toluene at 15.0 °C (previous data);[2] (◓) for a-PS in 4-*tert*-butyltoluene at 50.0 °C (previous data);[2] (□) for a-PS in cyclohexane at 36.0−45.0 °C (previous data).[3] The dotted and solid curves represent the values calculated from eqs 14 and 16 for α_H, respectively, and eq 15 for α_S.

the Yamakawa−Yoshizaki (YY) equation[26] for α_H, which takes account of the effect of fluctuating hydrodynamic interaction (HI) on the basis of the Gaussian chain, and eq 15 for α_S. The YY equation is explicitly given by

$$\alpha_H = \alpha_H^{(Z)} f_H \tag{16}$$

where $\alpha_H^{(Z)}$ is given by eq 14 and f_H is defined by

$$f_H = \frac{1 - \delta_{1,0}(1)}{1 - \delta_{1,0}(\alpha_S^{-1})} \tag{17}$$

with

$$\delta_{1,0}(x) = 0.12x^{0.43} \qquad (0 \le x \le 1) \tag{18}$$

Note that in eq 17 the ratio of the bead diameter to the effective bond length (for the Gaussian chain) has been taken as unity as in the previous papers.[2−4,26]

From Figure 5, it may be mentioned that the present data points for PIB in *n*-heptane form a single composite curve together with those for a-PS, but that strictly, the former points deviate slightly upward from the latter and are closer to the solid curve than the latter. We may therefore conclude that α_H becomes a function only of α_S within experimental error irrespective of the differences in polymer species and solvent condition. All the data points except for the PIB sample with the lowest α_S are located definitely below the dotted curve, and even below the solid curve, so that it is reconfirmed that the Barrett equation and also the YY equation overestimate α_H.

Next we examine the relation between α_H and α_η. The same data for α_H as in Figure 5 except those for a-PS in cyclohexane are double-logarithmically plotted against α_η in Figure 6. It also includes the data obtained by Fetters et al.[19] for PIB in *n*-heptane (triangles). Their values of α_H have been calculated from the values of R_H and $R_{H,\Theta}$ in Figure 3 and those for α_η have been calculated from their values of $[\eta]$ and $[\eta]_\Theta$ in *n*-heptane at 25.0 °C and in benzene at 25.0 °C (Θ), respectively.[19] Note that $[\eta]_\Theta$'s in IAIV at Θ and in benzene at Θ agree with each other for the PIB samples in the range of $M_w \gtrsim 10^5$. In the figure, the

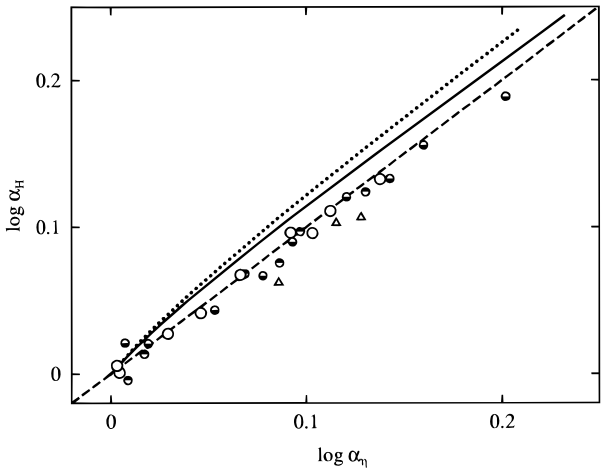

Figure 6. Double-logarithmic plots of α_H against α_η. The symbols have the same meaning as in Figure 5 except for the triangles, which represent the values due to Fetters et al.[19] for PIB in *n*-heptane at 25.0 °C. The dotted and solid curves represent the values calculated from eqs 14 and 16 for α_H, respectively, and eq 19 for α_η. The dashed line represents the relation $\alpha_H = \alpha_\eta$.

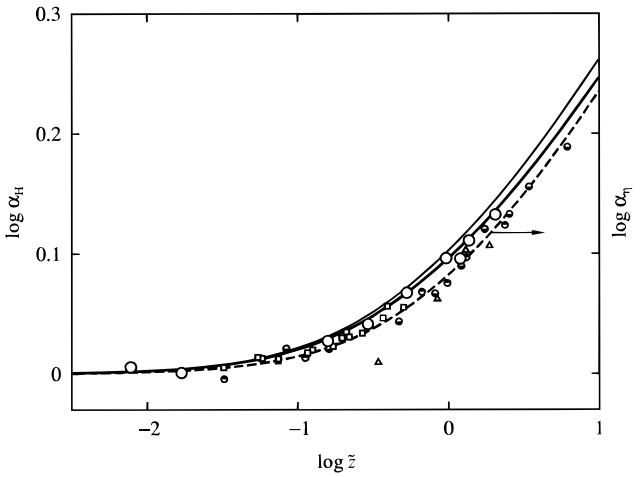

Figure 7. Double-logarithmic plots of α_H against $\tilde{z}$. The symbols have the same meaning as in Figures 5 and 6. The light and heavy solid curves represent the values of α_H calculated from eqs 14 and 16, respectively, with $\tilde{z}$ in place of z. The dashed curve represents the values of α_η calculated from eq 19 with $\tilde{z}$ in place of z.

dashed straight line represents the relation $\alpha_H = \alpha_\eta$, and the dotted and solid curves represent the values calculated from eqs 14 and 16 for α_H, respectively, and the Barrett equation[27] for α_η,

$$\alpha_\eta^{\,3} = (1 + 3.8z + 1.9z^2)^{0.3} \tag{19}$$

Note that for the theoretical values represented by the solid curve the effect of fluctuating HI has been taken into account only for α_H but not for α_η, as noted in the previous paper.[2]

As in Figure 5, the dotted curve in Figure 6 deviates significantly upward from the data points. The values of α_H represented by the solid curve are seen to be closer to the observed values but still larger than the latter. As in the case of a-PS in toluene and in 4-*tert*-butyltoluene,[2] it is found that the present data points also follow closely the dashed line, indicating that the relation $\alpha_H = \alpha_\eta$ holds also for PIB in *n*-heptane. The data points due to Fetters et al.[19] deviate somewhat downward from ours. In this connection, we note that all the current theories predict $\alpha_H > \alpha_\eta$.

α_H as a Function of $\tilde{z}$. Since the PIB chain is the most flexible of all polymers we have studied so far, the deviation of its α_H vs z plot due to chain stiffness from the conventional two-parameter theory prediction as given by eq 14 is not appreciable as in the case of the α_η vs z plot previously studied (see Figure 5 of ref 7). Thus, for PIB, we only examine the behavior of α_H as a function of the scaled excluded-volume parameter $\tilde{z}$.

According to the YSS theory,[9−11] the parameter $\tilde{z}$ as a function of the total contour length L of the HW chain is defined by

$$\tilde{z} = (3/4)K(\lambda L)z \tag{20}$$

and z is now given by

$$z = (3/2\pi)^{3/2}(\lambda B)(\lambda L)^{1/2} \tag{21}$$

where

$$B = \beta/a^2 c_\infty^{\,3/2} \tag{22}$$

with β the binary-cluster integral between beads, a their spacing (effective bond length), and c_∞ being given by eq 9. In eq 20, the coefficient $K(L)$ is given by

$$K(L) = \frac{4}{3} - 2.711L^{-1/2} + \frac{7}{6}L^{-1} \text{ for } L > 6$$
$$= L^{-1/2}\exp(-6.611L^{-1} + 0.9198 + 0.03516L) \text{ for } L \le 6 \tag{23}$$

Then L is related to the degree of polymerization x by the equation

$$L = xM_0/M_L \tag{24}$$

where M_0 is the molecular weight of the repeat unit of a given real chain.

Figure 7 shows double-logarithmic plots of α_H against $\tilde{z}$ with the same data as those in Figures 5 and 6. Here, the values of $\tilde{z}$ have been tentatively calculated as before[7] with $\lambda^{-1} = 12.7$ Å determined from $[\eta]_\Theta$[14] (the value given in the second row of Table 5), $\lambda B = 0.083$ determined from α_S,[7] and $M_L = 24.1$ Å^{-1}, assuming that the PIB chain may be represented by the KP wormlike chain taking as its contour the helix axis of the 8_3 helix in the crystalline state. The light solid curve represents the values of α_H calculated from eq 14, and the heavy solid curve represents those calculated from eq 16 with eqs 14 (for $\alpha_H^{(Z)}$), 15, 17, and 18, both with $\tilde{z}$ in place of z. The dashed curve represents the values of α_η calculated from eq 19 with $\tilde{z}$ in place of z. It is seen that all the data points except the lowest of those due to Fetters et al. form a single composite curve, which may be identified with the dashed curve, within experimental error, although the present data points for PIB in *n*-heptane deviate somewhat upward and are closer to the heavy solid curve than to the dashed curve. The implication is that α_H becomes a function only of $\tilde{z}$ (within experimental error) irrespective of the differences in polymer species and solvent condition; or, in other words, the QTP scheme may be valid also for α_H as well as for α_S and α_η.

As pointed out in the previous papers[2−4] and anticipated from the results in Figure 5, the light solid curve deviates upward progressively from the data points with increasing $\tilde{z}$. The deviation is decreased by taking

account of the effect of fluctuating HI, as shown by the heavy solid curve.

Concluding Remarks

We have investigated the unperturbed and perturbed hydrodynamic radii $R_{H,\Theta}$ and R_H for PIB in IAIV at 25.0 °C (Θ) and in *n*-heptane at 25.0 °C, respectively. As was expected from the previous result that the values of the unperturbed and perturbed intrinsic viscosities $[\eta]_\Theta$ and $[\eta]$ for PIB agree with each other in the oligomer region,[7] it has been found that the values of $R_{H,\Theta}$ and R_H also agree with each other in the same region. We have therefore been able to determine the hydrodynamic-radius expansion factor α_H by simply adopting the values of $R_{H,\Theta}$ as the unperturbed values $R_{H,0}$ in *n*-heptane. We have analyzed the data for $R_{H,\Theta}$ (or D_Θ) itself as usual by the use of the corresponding (unperturbed) HW theory to determine λ^{-1}. The result is larger than the value previously obtained from $[\eta]_\Theta$, as in the cases of the other polymers studied so far.[15,17,18,23]

With the previous results for α_S and α_η for PIB in *n*-heptane at 25.0 °C, we have examined the behavior of α_H as a function of α_S, α_η, or $\tilde{z}$. It has then been found that the data points for α_H as a function of α_S, α_η, or $\tilde{z}$ form a single composite curve together with the corresponding previous results for a-PS[1−3,7] within experimental error over the whole range of M_w studied. This reconfirms that the QTP scheme may be valid for α_H as well as for α_S and α_η irrespective of the differences in chain stiffness, local conformation, and solvent condition. Strictly, however, the data points for α_H and also α_η as functions of $\tilde{z}$ for our PIB deviate somewhat upward from the respective single composite curves for a-PS, although the relation $\alpha_H = \alpha_\eta$ holds (see ref 7 for α_η). This suggests that $\langle S^2\rangle_0$ in *n*-heptane at 25.0 °C is somewhat different from $\langle S^2\rangle_\Theta$ in IAIV at Θ. An investigation of this point is one of the problems in the future.

The present results for PIB give the values of α_H smaller than those calculated from the Barrett equation,[24] being consistent with the previous results for a-PS[2,3] and PDMS.[4] It has been again found that the Yamakawa−Yoshizaki theory gives the right direction for the effect of fluctuating hydrodynamic interaction on α_H.

For the further confirmation of the validity of the QTP scheme for α_H, we make a similar study for atactic and isotactic poly(methyl methacrylate)s in the following paper.[28]

References and Notes

(1) Abe, F.; Einaga, Y.; Yoshizaki, T.; Yamakawa, H. *Macromolecules* **1993**, *26*, 1884; and succeeding papers.
(2) Arai, T.; Abe, F.; Yoshizaki, T.; Einaga, Y.; Yamakawa, H. *Macromolecules* **1995**, *28*, 3609.
(3) Arai, T.; Abe, F.; Yoshizaki, T.; Einaga, Y.; Yamakawa, H. *Macromolecules* **1995**, *28*, 5458.
(4) Horita, K.; Sawatari, N.; Yoshizaki, T.; Einaga, Y.; Yamakawa, H. *Macromolecules* **1995**, *28*, 4455.
(5) Abe, F.; Horita, K.; Einaga, Y.; Yamakawa, H. *Macromolecules* **1994**, *27*, 725.
(6) Kamijo, M.; Abe, F.; Einaga, Y.; Yamakawa, H. *Macromolecules* **1995**, *28*, 1095.
(7) Abe, F.; Einaga, Y.; Yamakawa, H. *Macromolecules* **1993**, *26*, 1891.
(8) Horita, K.; Abe, F.; Einaga, Y.; Yamakawa, H. *Macromolecules* **1993**, *26*, 5067.
(9) Yamakawa, H.; Stockmayer, W. H. *J. Chem. Phys.* **1972**, *57*, 2843.
(10) Yamakawa, H.; Shimada, J. *J. Chem. Phys.* **1985**, *83*, 2607.
(11) Shimada, J.; Yamakawa, H. *J. Chem. Phys.* **1986**, *85*, 591.
(12) Yamakawa, H. *Annu. Rev. Phys. Chem.* **1984**, *35*, 23.
(13) Yamakawa, H. In *Molecular Conformation and Dynamics of Macromolecules in Condensed Systems*; Nagasawa, M., Ed.; Elsevier: Amsterdam, 1988; p 21.
(14) Abe, F.; Einaga, Y.; Yamakawa, H. *Macromolecules* **1991**, *24*, 4423.
(15) Yamada, T.; Koyama, H.; Yoshizaki, T.; Einaga, Y.; Yamakawa, H. *Macromolecules* **1993**, *26*, 2566.
(16) Konishi, T.; Yoshizaki, T.; Yamakawa, H. *Macromolecules* **1991**, *24*, 5614.
(17) Yamada, T.; Yoshizaki, T.; Yamakawa, H. *Macromolecules* **1992**, *25*, 377.
(18) Dehara, K.; Yoshizaki, T.; Yamakawa, H. *Macromolecules* **1993**, *26*, 5137.
(19) Fetters, L. J.; Hadjichristidis, N.; Lindner, J. S.; Mays, J. W.; Wilson, W. W. *Macromolecules* **1991**, *24*, 3127.
(20) Yamakawa, H.; Yoshizaki, T. *J. Chem. Phys.* **1983**, *78*, 572.
(21) Kratky, O.; Porod, G. *Recl. Trav. Chim.* **1949**, *68*, 1106.
(22) Kusanagi, H.; Tadokoro, H.; Chatani, Y. *Polym. J.* **1977**, *9*, 181.
(23) Sawatari, N.; Konishi, T.; Yoshizaki, T.; Yamakawa, H. *Macromolecules* **1995**, *28*, 1089.
(24) Barrett, A. J. *Macromolecules* **1984**, *17*, 1561.
(25) Domb, C.; Barrett, A. J. *Polymer* **1976**, *17*, 179.
(26) Yamakawa, H.; Yoshizaki, T. *Macromolecules* **1995**, *28*, 3604.
(27) Barrett, A. J. *Macromolecules* **1984**, *17*, 1566.
(28) Arai, T.; Sawatari, N.; Yoshizaki, T.; Einaga, Y.; Yamakawa, H. *Macromolecules* **1996**, *29*, 2309.

MA951273V